Vibrational Spectra and Structures of Nickel Mononitrosyl Complexes. An IR Matrix Isolation and DFT Study

Lahouari Krim,* Laurent Manceron, and M. Esmaïl Alikhani

LADIR/Spectrochimie Moléculaire, UMR CNRS−P6, Université Pierre et Marie Curie, Bat F74, Boîte 49, 4 place Jussieu, 75252 Paris, Cedex 05, France

Received: November 9, 1998; In Final Form: February 15, 1999

The infrared spectra of nickel mononitrosyl complexes isolated in solid argon at low temperature have been reinvestigated. Concentration and photochemical studies demonstrate the existence of two isomeric forms of NiNO. Analyses of the $^{58}Ni/^{60}Ni$, $^{14}N/^{15}N$, and $^{16}O/^{18}O$ isotopic effects indicate that a first form has an end-on bent configuration, and a second form has a cyclic structure, in which the NO ligand is significantly more perturbed. Density functional calculations of the geometrical, electronic and vibrational properties of these two forms are also presented and compared to the experimental values. Isomerization energies have been estimated.

1. Introduction

Coordinatively saturated, zerovalent transition metal (TM) mononitrosyl compounds, such as $Mn(CO)_4NO$, $Co(CO)_3NO$, or $(C_5H_5)NiNO$, are long known and their geometries well established.[1−5] In these compounds the different electronic structures of nitrosyl and carbonyl groups do not lead to drastic discrepancies in the molecular shapes, in comparison with isolectronic penta and tetracarbonyl compounds. The nitrosyl group is bound to the TM atomic with an end-on configuration with linear M−NO arrangements and perhaps slightly shorter M−N than M−C bond distances.

In larger nickel mononitrosyl systems involving stabilizing coligands (mainly halogens and substituted phosphines), a number of structural determinations indicate the existence of various coordination modes ranging from linear to slightly bent (160° or greater) and truly bent (119 to 130°).[6] It has been suggested to associate the various geometries of the Ni−NO fragment to the different oxidation states of the nitrosyl group, in a formal sense, which would vary from cationic NO^+ − type in linear or quasi linear arrangements to anionic NO^- species in highly bent systems.[6] IR studies trying to link the changes in the NO stretching frequency (ν_{NO}) to the changes in geometry and, presumably, electronic structure are made difficult by the parameter sensitivity to concomitant changes in the nature of the coligands involved. In that sense, studies on isolated metal mononitrosyl are of interest. These species are, of course, more elusive, being coordinatively unsaturated and thus highly reactive triatomics. Gas-phase studies have so far brought out TM − NO bimolecular reaction rates or estimates of activation energies.[7] Matrix isolation spectroscopic studies and ab initio predictions can bring direct insight into the structure of these intermediate complexes. Two studies have been published recently concerning the NiNO species, among various first-row transition metal nitrosyl triatomics.[8,9] The first study by Ruschel et al. combines both methods to identify two possible isomeric form or electronic states, reportedly corresponding to ν_{NO} stretching frequencies at 1727 and 1676 cm^{-1}. Both studies include DFT calculations and predict similar ground-state geometries (bent structure with Ni−NO bond angle equal to about 136°).

In the course of preliminary studies involving reactions of Ni atoms and NO molecules performed in this laboratory, it appeared that the absorptions reported earlier could not all belong to nickel mononitrosyl species. This prompted us to reinvestigate this system, with an additional effort to observe the low-frequency stretching and bending vibrations, which are sensitive markers of the metal−ligand interaction.[10,11] The structural and vibrational study of the complex has also been carried out using the density functional theory approach (DFT).

2. Experimental and Theoretical Techniques

The NiNO samples were prepared by cocondensing Ni vapor and NO/Ar mixtures (0.2 to 2% molar ratios) onto a cryogenic metal mirror maintained around 10K. The experimental methods and setup have been previously described.[11,12] Briefly, here, Ni was vaporized from a tungsten filament wetted with nickel and heated resistively to ∼1500 °C. Metal deposition rates, monitored with a microbalance, were typically of the order of 0.25−0.75 μg/min. Deposition times were around 120 min and, typically, 1.5 mmol of the gaseous mixture were deposited.

Argon gas, was furnished by L'Air liquide with a purity of 99.9995%. ^{14}NO gas was also provided by L'Air Liquide with a stated chemical purity of 99.9%, ^{15}NO gas by Isotec with an isotopical purity of 97.8%. $^{14}N^{18}O$ was prepared in the laboratory by addition of $^{18}O_2$ onto $^{14}N^{16}O$ gas to form $^{14}N^{(16+18)}O_2$ which was subsequently reduced to $^{14}N^{18}O$ and $^{14}N^{116}O$ by reaction with mercury.[13] The resulting gas is a mixture containing approximately 52% $^{14}N^{16}O$ and 48% $^{14}N^{18}O$. NO gas and its isotopomers were purified, to remove N_2, N_2O and NO_2, by using trap-to-trap vacuum distillations. The purity of samples was confirmed spectroscopically.

Spectra were recorded using a FTIR Bruker spectrometer (IFS 120HR) at 0.5 cm^{-1} resolution in the 20−6000 cm^{-1} range. A Hg Lamp was used for the domain located below 100 cm^{-1} and Globar above 100 cm^{-1}. A Bolometer detector and 23 and 6 μm Mylar beam splitters were used for the low frequency region, typically from 20 to 700 cm^{-1}, a HgCdTe detector from 700 to 3000 cm^{-1}, and a InSb detector from 2000 to 6000 cm^{-1}. No signal was observed below 100 cm^{-1} and beyond 3750 cm^{-1}, under the present conditions.

* To whom correspondence should be sent. E-mail: Krim@ccr.jussieu.fr.

10.1021/jp984352s CCC: $18.00
Published on Web 04/15/1999

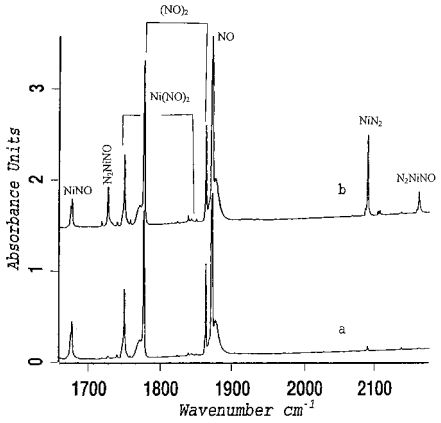

Figure 1. Infrared absorption spectra of nickel and NO-containing complexes. NO, N_2, and Ni trapped in argon matrix at 10 K, 1630−2200 cm^{-1} region (a) Ni:$^{14}N^{16}O$/Ar = 0.5:1/100, (b) Ni:$^{14}N^{16}O$:N_2/Ar = 0.5:1:1/100.

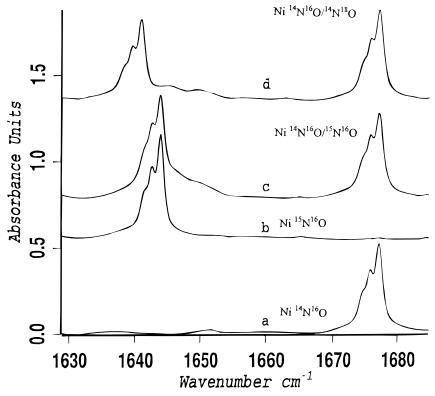

Figure 2. NO and Ni trapped in argon matrix at 10 K, 1630−1690 cm^{-1} region (ν_1 of $^2A'$ NiNO) (a) Ni:$^{14}N^{16}O$/Ar = 0.5:1/100, (b) Ni:$^{15}N^{16}O$/Ar = 0.5:1/100, (c) Ni:^{14}NO:$^{15}N^{16}O$/Ar = 0.5:1:1/100, (d) Ni:^{14}NO:$^{14}N^{18}O$/Ar = 0.5:1:1/100.

For each sample, corresponding to different concentrations of Ni and NO, or different isotopic precursors, four kinds of spectra were recorded at 10 K, after each of the following procedures: (i) after sample deposition, (ii) after warming up the matrix at several steps up to 35 K in order to vary and monitor the formation of higher stoechiometry complexes, (iii) after irradiating the sample using a 200 W mercury−xenon high-pressure arc lamp and interference filters centered at various wavelength ranges (436, 240 and 220 nm), (iv) after warming up the photolyzed matrix at several steps up to 35 K.

Density Functional Theory (DFT) calculations have been performed on the NiNO system using the Gaussian 94 quantum chemical package.[14] Two pure DFT methods and two hybrid functionals were used. In all cases Becke's gradient-corrected exchange functional[15] was combined either with the gradient-corrected correlation functional of Lee, Yang, and Parr[16] (denoted as BLYP and B3LYP) or with the gradient-corrected functional of Perdew-Wang 91 [17] (denoted as BPW91 and B3PW91). The 6-311+G(2d) extended basis set of Pople et al.[18] has been used for oxygen and nitrogen. For Ni, the basis set of Schaefer et al.[19] with triple-ζ quality in the valence region (17s10p6d)/^{6s3p3d} was chosen.

3. Experimental Results

Infrared spectra of samples formed by the codeposition of Ni and NO in argon matrixes revealed that some contradictions with those presented, for the similar experiment, by Ruschel et al.[8] On one hand, there are new absorptions in other spectral regions, in addition to the observed bands in the N−O stretching region (1600−1800 cm^{-1}). On the other hand, in this latter spectral region, five strong bands located at 1872, 1863.4, 1776.3, and 1749.8 and 1677.1 cm^{-1}, (Figure 1a). These have already been attributed to NO monomer,[12,20] N−O symmetric and asymmetric stretching in $(NO)_2$,[12,14] N−O stretching in $Ni(NO)_2$, and NiNO complexes,[8] respectively. No band was found at 1727.3 cm^{-1} under these conditions, which contradicts the experimental observations made by Ruschel et al. A matrix formed by the codeposition of Ni and NO/N_2/Ar = 1/1/100 reveals, however, three other strong bands, located at 1727.4, 2089.5, and 2165.1 cm^{-1} (Figure 1b). The band located at 2089.5 is the N−N stretching mode of the NiN_2 complex (ν_1).[11] The intensities of the two other bands located at 1727.4 and 2165.1 cm^{-1} depend on both Ni, NO and N_2 concentrations and they are also sensitive to the NO isotopic substitution. According to the relative concentration effects, these two bands could be attributed to a (NO)Ni(N_2) ternary complex.

Note that when NO gas is used without further purification impurities as NO_2, N_2O and N_2 are present in thermodynamical equilibrium and can induce the formation of ternary species.

Concentration and Temperature Effects. In this paper we shall focus our study on the NiNO triatomic, another work will be devoted to $Ni(NO)_2$ complex,[21] for which more than six vibrational modes have been detected.

Six bands corresponding to 1:1 stoichiometries, NiNO complexes have been observed. They have the same behavior when the NO and Ni concentrations are changed and appear as doublets in spectra obtained with NO isotopic mixtures ($^{14}N^{16}O$/$^{15}N^{16}O$ or $^{14}N^{16}O$/$^{14}N^{18}O$). Their relative infrared intensities remain constant after warming the matrix up to 35 K. The measured frequencies of $Ni^{14}N^{16}O$ complexes and their isotopomers ($Ni^{15}N^{16}O$, $Ni^{14}N^{18}O$) are listed in Table 1.

In addition to the strong band at 1677.1 cm^{-1} in the NO stretching spectral region (Figure 2) corresponding to the NiNO complex and that has already been observed by Ruschel et al., another sharp absorption at 1293.8 cm^{-1} (Figure 3) was detected, whose infrared intensity is about 6.5 times less intense than the former band. The band observed at 3324.3 cm^{-1} (Figure 4) is consistent with the overtone of the band located at 1677.1 cm^{-1}. The integrated intensity for 3324.3 cm^{-1} is about 36 times

TABLE 1: Observed Frequencies in cm^{-1} (Relative Intensities Are in Parentheses) of $Ni^{14}N^{16}O$, $Ni^{15}N^{16}O$, and $Ni^{14}N^{18}O$ Complexes Isolated in Argon Matrix

$^{58}Ni^{14}N^{16}O$	$^{60}Ni^{14}N^{16}O$	$^{58}Ni^{15}N^{16}O$	$^{60}Ni^{15}N^{16}O$	$^{58}Ni^{14}N^{18}O$	$^{60}Ni^{14}N^{18}O$
464.4 (7.7×10^{-3})		461.8		446.9	
540.5 (1.4×10^{-3})	537.9	528.9	527.1	537.2	
608.4 (0.012)	605.2	600.7	597.6	596.7	593.8
1293.8 (0.155)		1271.5		1260.3	
1677.1 (1)[a]		1643.9		1640.9	
3324.3 (0.028)		3258.9		3252.4	

[a] The relative IR intensity is calculated with respect to the 1677.1 cm^{-1} band.

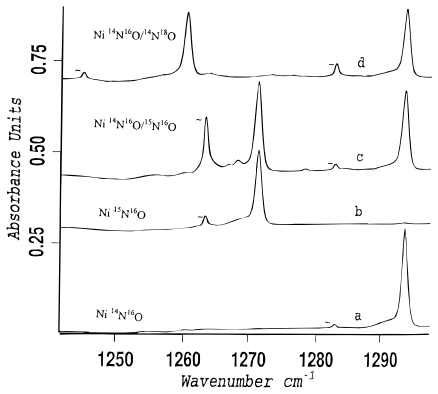

Figure 3. NO and Ni trapped in argon matrix at 10 K, 1240−1300 cm^{-1} region (ν_1 of ^{2}A" NiNO) (a) Ni:$^{14}N^{16}O$/Ar = 0.5:1/100, (b) Ni:$^{15}N^{16}O$/Ar = 0.5:1/100, Ni:^{14}NO:$^{15}N^{16}O$/Ar = 0.5:1:1/100, (d) Ni:^{14}NO:$^{14}N^{18}O$/Ar = 0.5:1:1/100. Peaks labeled ~ belong to N_2O isotopomers represent a inpurities in NO.

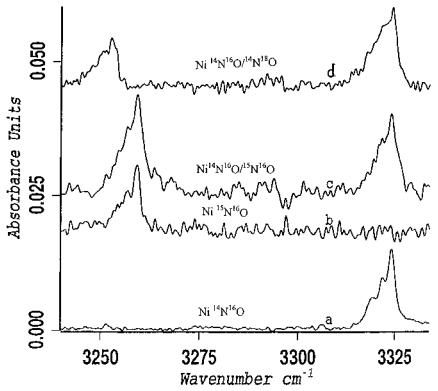

Figure 4. NO and Ni trapped in argon matrix at 10 K, 3220−3330 cm^{-1} region ($2\nu_1$ of ^{2}A′ NiNO) (a) Ni:$^{14}N^{16}O$/Ar = 0.5:1/100, (b) Ni:$^{15}N^{16}O$/Ar = 0.5:1/100, (c) Ni:^{14}NO:$^{15}N^{16}O$/Ar = 0.5:1:1/100, (d) Ni:^{14}NO:$^{14}N^{18}O$/Ar = 0.5:1:1/100.

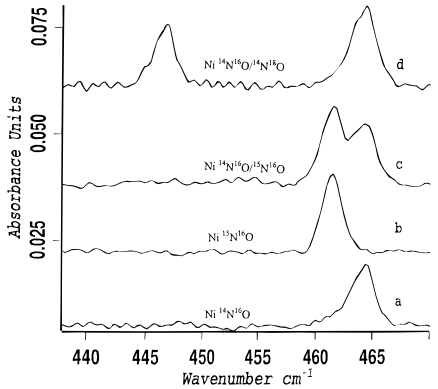

Figure 5. NO and Ni trapped in argon matrix at 10 K, 400−480 cm^{-1} region (ν_3 of ^{2}A" NiNO) (a) Ni:$^{14}N^{16}O$/Ar = 0.5:1/100, (b) Ni:$^{15}N^{16}O$/Ar = 0.5:1/100, (c) Ni:^{14}NO:$^{15}N^{16}O$/Ar = 0.5:1:1/100, (d) Ni:^{14}NO:$^{14}N^{18}O$/Ar = 0.5:1:1/100.

smaller than that of the fundamental band, and the isotopic shifts ($^{14}N/^{15}N$, $^{16}O/^{18}O$) are nearly twice the shifts observed for the corresponding fundamental band. From the knowledge of fundamental and overtone frequencies, anharmonicities have been evaluated at 14.95, 14.45, and 14.7 cm^{-1} for Ni$^{14}N^{16}O$, Ni$^{15}N^{16}O$, and Ni$^{14}N^{18}O$, respectively.

In the far-infrared region three absorption bands have been observed at 464.4, 540.5, and 608.4 cm^{-1} (Figures 5−7). The two latter bands are doublets. The intensity ratio of the

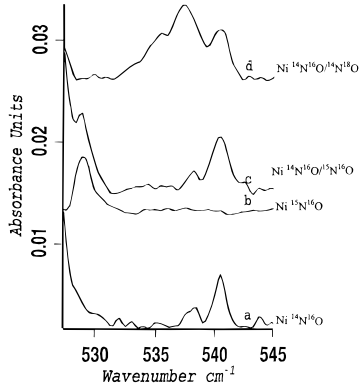

Figure 6. NO and Ni trapped in argon matrix at 10 K, 520−550 cm^{-1} region (ν_2 of ^{2}A" NiNO) (a) Ni:$^{14}N^{16}O$/Ar = 0.5:1/100, (b) Ni:$^{15}N^{16}O$/Ar = 0.5:1/100, (c) Ni:^{14}NO:$^{15}N^{16}O$/Ar = 0.5:1:1/100, (d) Ni:^{14}NO:$^{14}N^{18}O$/Ar = 0.5:1:1/100.

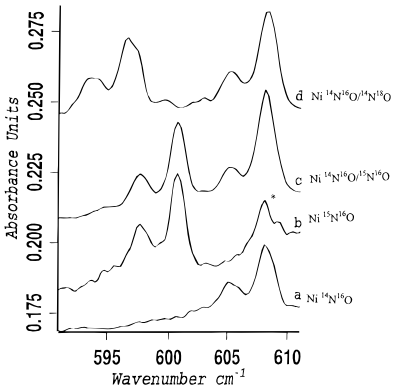

Figure 7. NO and Ni trapped in argon matrix at 10 K, 590−610 cm^{-1} region (ν_2 of ^{2}A′ NiNO) (a) Ni:$^{14}N^{16}O$/Ar = 0.5:1/100, (b) Ni:$^{15}N^{16}O$/Ar = 0.5:1/100, (c) Ni:^{14}NO:$^{15}N^{16}O$/Ar = 0.5:1:1/100, (d) Ni:^{14}NO:$^{14}N^{18}O$/Ar = 0.5:1:1/100. Peak labeled * belong to Ni(NO)$_2$.

components, which make up the doublet, is in good agreement with the natural isotopic ratio $^{58}Ni/^{60}Ni$ (2.6) and is unaffected by any change in experimental conditions (temperature, concentrations). This doublet structure is thus probably due to the Ni isotopic composition (^{58}Ni ~ 68% and ^{60}Ni ~ 26%).

Photolysis Effects. NiNO is a triatomic system, but we detect here five fundamental bands. These bands have the same behavior when the matrix is annealed, as well as when the Ni or NO concentrations and NO isotopic compositions are varied. Their intensity ratio also remain constant when impurities such as O_2, N_2, N_2O, CO, and CO_2 are added to the matrix, thus indicating that these belong to NiNO species. However it is possible to separate these five bands into two groups of two and three bands, using selective photoirradiations. First, the sample was irradiated for more than 30 min using a 200 W mercury−xenon high-pressure arc lamp without any interference filter. Infrared spectra of the photolyzed sample show that intensities of the five bands decreased of about 50%. This photodissociation of the NiNO complex was accompanied by other phenomena as new photoproducts absorptions (insertion reaction that requires activation energy to give a more stable NNiO product) or self-association of NO to increase absorptions of $(NO)_2$ and Ni$(NO)_2$ complexes.[21]

Spectra obtained using a selective photoirradiation at 436 nm show that intensities of the three bands located at 464.4, 540.5, and 1293.8 cm^{-1} (set A) decreased while these of the two other bands left, located at 608.4 and 1677.1 cm^{-1} (set B), increased. The reverse phenomenon was observed with the irradiation wavelength at 240 nm, where intensities of the first set of bands

TABLE 2: Observed and Calculated[a] Frequencies (cm^{-1}) of the Various Isotopic Species of NiNO (A)[b]

$^{58}Ni^{14}N^{16}O$		$^{60}Ni^{14}N^{16}O$		$^{58}Ni^{15}N^{16}O$		$^{60}Ni^{15}N^{16}O$		$^{58}Ni^{14}N^{18}O$		$^{60}Ni^{14}N^{18}O$		
obsd	calcd	obsd	calcd	obsd	calcd	obsd	calcd	obsd	calcd	obsd	calcd	
464.4	464.7	*c*		461.8	461.9	*c*		446.9	445.1	*c*		ν_3
540.5	540.6	537.9	538.3	528.9	528.9	527.1	526.4	537.2	537.9	*c*		ν_2
1293.8	1293.8	*c*	1293.6	1271.5	1270.9	*c*	1270.7	1260.3	1260.4	*c*	1260.4	ν_1

[a] The force constants are $F_{NO} = 6.57$ mdyn Å^{-1}, $F_{NiN} = 2.19$ mdyn Å^{-1}, $F_{NiO} = 1.91$ mdyn Å^{-1}, $F_{NO,NiN} = 0.59$ mdyn Å^{-1}, $F_{NiN,NiO} = 0.08$ mdyn Å^{-1}, and $F_{NiO,NO} = 0.90$ mdyn Å^{-1}. [b] The geometric parameters of the first species NiNO (A) are $r_{NO} = 1.22$ Å, $r_{NiN} = 2$ Å and ∠NiNO = 70°. [c] $^{58}Ni/^{60}Ni$ effects are unresolved.

TABLE 3: Observed and Calculated[a] Frequencies (cm^{-1}) of the Various Isotopic Species of NiNO (B)[b]

$^{58}Ni^{14}N^{16}O$		$^{60}Ni^{14}N^{16}O$		$^{58}Ni^{15}N^{16}O$		$^{60}Ni^{15}N^{16}O$		$^{58}Ni^{14}N^{18}O$		$^{60}Ni^{14}N^{18}O$		
obsd	calcd	obsd	calcd	obsd	calcd	obsd	calcd	obsd	calcd	obsd	calcd	
c		*c*		*c*		*c*		*c*		*c*		ν_3
608.4	608.4	605.2	605.2	600.7	600.7	597.6	597.5	596.7	597.0	593.8	593.9	ν_2
1677.1	1677.1	*d*	1677.0	1643.9	1643.8	*d*	1643.0	1640.9	1640.5	*d*	1640.3	ν_1

[a] The force constants are $F_{NO} = 11.42$ mdyn Å^{-1}, $F_{NiN} = 4.45$ mdyn Å^{-1}, $F_{NiNO} = 0.76$ mdyn Å rad^{-2}, $F_{NO,NiN} = -0.24$ mdyn Å^{-1}, $F_{NO,NiNO} = 0.75$ mdyn rad^{-1}, $F_{NiN,NiNO} = 0.90$ mdyn rad^{-1}. [b] The geometric parameters of the second species NiNO (B) are $r_{NO} = 1.198$ Å, $r_{NiN} = 1.689$ Å, and ∠NiNO = 135.6°. [c] The ν_3 mode was not experimentally detected. [d] $^{58}Ni/^{60}Ni$ effects are unresolved.

increased and those of the second set of bands decreased. Photodissociation of the NiNO complexes was observed when the sample was irradiated at 220 nm. These phenomena of intensity inversion of two groups of NiNO complex bands, show that there are two kinds of isomeric forms NiNO, having the same stoichiometry.

Vibrational Analysis. The products of the nitric oxide cocondensation reactions with Ni, as described previously, showed that there are two NiNO species: NiNO (A) and NiNO (B). The large differences in spectral characteristics between the two forms are indicative of large difference in geometrical and bonding properties.

To bring more information about bonding properties and molecular shapes of these two NiNO (A) and (B) isomers, semiempirical harmonic force field calculations were performed based on several geometries. For both forms, a NiNO linear configuration is to be excluded, because of the large difference between the experimental and calculated isotopic shifts (the errors on the calculated isotopic shifts exceeds 14%, at best, and this requires that some force constants take completely unrealistic values).

The first species (A) has three absorption bands located at 464.4, 540.5, and 1293.8 cm^{-1}. Measured shifts of the low frequency 464.5 cm^{-1} band are about 2.6 and 17.5 cm^{-1} for $Ni^{15}N^{16}O$ and $Ni^{14}N^{18}O$, respectively. In any configuration corresponding to an end-on coordination on the nitrogen atom (with the ∠NiNO bond angle varying between 180 and 90°), the largest ratio between $^{16}O/^{18}O$ and $^{14}N/^{15}N$ shifts is found for the case of a low frequency stretching mode, for a hypothetical linear arrangement. Even then, this ratio is computed to be 2.5, while it is measured here about 6.7. Only for structures involving Ni bonded to the oxygen, vibrational isotopic effects on the order of that experimentally observed can be calculated. For this species the best fit was obtained as long as the NiNO angle is close to 70 ± 3° (the NiNO bond angle varied stepwise between 180 and 20°). The internuclear distance NiN was taken around the given value (1.689 Å) for NiN_2 complex.[11] The NO, NNi and NiO interatomic distances have been chosen as internal coordinates (because the NiO and NiN internuclear distances are close to each other), correlating in a first approximation to the normal coordinates associated to the ν_1, ν_2, and ν_3 frequencies, respectively. For one given geometry (∠NiNO = 70°), a set of force constants that gives a good agreement between the observed and calculated frequencies (the average errors on the calculated isotopic shifts is less than 0.2%) is presented in Table 2. The NO force constant is of the order of 6.57 mdyn Å^{-1}, about 2.4 times smaller than that for NO monomer (16 mdyn Å^{-1}), which explains the large red shift (578.4 cm^{-1}) of the NO stretching mode for this species. The NiN force constant is around 2.19 mdyn Å^{-1}, only 1.15 times larger than that associated to the NiO coordinate, but about 1.6 times smaller than that of NiN in NiN_2 complex (3.6 mdyn Å^{-1}).[11] The NO, NiN, and the NO, NiO interaction force constants have relatively large values of 0.59 and 0.9 mdyn Å^{-1}, respectively.

For the second species NiNO (B), observed and calculated frequencies are in good agreement (with average errors on the calculated isotopic shifts less than 0.01%), as long as the angle ∠NiNO is kept close to 133 ± 3° (the NiNO bond angle was also varied stepwise between 180 and 20°). The force field calculations presented below were performed based on the BLYP geometry.[8] The internal coordinates are chosen as NO and NiN stretches and the NiNO bond angle, corresponding in a first approximation to the normal coordinated corresponding to the ν_1, ν_2 stretching modes, and ν_3 bending mode, respectively. The force constants giving the best fit of experimental data are listed in Table 3. For this species the bending mode was not experimentally detected. If the normal mode associated to the ν_1 vibration involves primarily the NO internal coordinate, calculations of the $^{14}N/^{15}N$ and $^{16}O/^{18}O$ isotopic shifts show that the ν_2 mode must involve a mixture of the NiN and NiNO angle coordinates (about 80 and 17%, respectively in the potential energy distribution). This is possible only if the ν_3 frequency lies not too far below, that is, for the F_{NiNO} bond angle constants values between 0.7 and 0.8 mdyn Å rad^{-2}. The NO force constant is of order of 11.42 mdyn Å^{-1}, about 1.7 times larger than that of NO in NiNO (A) species. The NiN force constant is 4.45 mdyn Å^{-1}, about twice as large as that in the NiNO (A) species. Note that, in order to reproduce the experimental isotopic effects, the NO,NiN interaction force constant must be negative with this geometry, in contrast to that of the nickel carbonyl and dinitrogen species, where it has a large positive value.[10,11] Physically this would mean that, near the equilibrium structure, lengthening the NO bond tends to lengthen the Ni−N distance as well, or else that the lengthening of the NO bond distance upon formation of the nickel nitrosyl coordination bond goes through a minimum before the equilibrium structure.

Finally, it should be noticed that for both A and B species, some parallels can be made with previous studies on metal

TABLE 4: Summary of Results for NO and Ni

parameters	B3LYP	B3PW91	BLYP	BPW91	exptl[a]
NO ($^2\Pi$)					
r (Å)	1.1474	1.1447	1.1645	1.1600	1.1508
ω (cm^{-1})	1955.8	1982.9	1827.9	1867.6	1904.2[b] (1872.2[c])
μ (D)	0.13	0.15	0.18	0.2	0.15
E (au)	−129.934266	−129.879245	−129.927801	−129.928951	
Ni (^{3}D)					
E_{Ni} (au)	−1508.299366	−1508.251951	−1508.353923	−1508.429312	

[a] Reference 24. [b] Harmonic frequency. [c] Experimental value in matrix (this work).

TABLE 5: Energetical, Geometrical and Vibrational Properties of NiNO (^{2}A′)[a]

parameters	B3LYP	B3PW91	BLYP	BPW91	exptl[a]
r (N−O) (Å)	1.1841	1.1797	1.1933	1.1877	
r_1 (N−Ni) (Å)	1.7013	1.6872	1.6686	1.6550	
∠(NiNO) (deg)	134.7	135.5	138.2	138.2	
μ (D)	2.8	2.8	2.0	2.0	
E(au)	−1638.292191	−1638.191268	−1638.370999	−1638.545900	
D_e (kcal/mol)[b]	−36.5	−37.7	−56.0	−60.6	
ω_3 (cm^{-1})	241.8	243.8	259.6	258.6 (0.009)	
ω_2 (cm^{-1})	542.9	551.1	658.0	673.4 (0.04)	608.4 (0.012)
ω_1 (cm^{-1})	1699.0	1735.1	1638.4	1684.4 (1)	1677.1 (1)
$\delta_{\omega 1}$ (cm^{-1})[c]	256.8	247.8	189.5	183.2	195.1

[a] The frequencies are in cm^{-1}. Relative infrared intensities reported in parentheses are calculated with respect to the infrared intensity of the N−O stretching mode. [b] $D_e = E$(submolecules) − E(complex). [c] $\delta_\omega = \omega$ (isolated molecule) − ω (complexed molecule).

TABLE 6: Energetical, Geometrical, and Vibrational Properties of NiNO (^{2}As″) and NiNO (TS)[a]

	NiNO (^{2}A″)			NiNO (TS)
parameters	B3PW91	BPW91	exptl[a]	B3PW91
r (N−O) (Å)	1.2520	1.2759		1.2232
r_1 (N−Ni) (Å)	1.8178	1.7880		1.8241
∠(NiNO) (deg)	73.0	72.8		96.0
μ (D)	4.9	4.7		4.2
E (au)	−1638.173067	−1638.421327		−1638.166806
D_e (kcal/mol)	−26.3	−39.6		−22.3
ω_3 (cm^{-1})	378.7	418.9 (0.006)	464.4 (0.008)	277.7i
ω_2 (cm^{-1})	494.2	573.1 (0.005)	540.5(0.0014)	522.5
ω_1 (cm^{-1})	1385.9	1297.9 (0.1)	1293.8 (0.16)	1469.7
$\delta_{\omega 1}$ (cm^{-1})	597.0	569.7	578.4	

[a] See legends of Table 5.

mononitrosyl complexes. On one hand, Chiarelli et al.[22] detected for the $Cu^{14}N^{16}O$ complex, the Cu−N stretching mode at 608.8 cm^{-1} and the N−O stretching mode at 1610.5 cm^{-1}, which is comparable with the experimental data of NiNO (B) species. On the other hand, Andrews et al.[23] measured the N−O stretching mode of the Li^+ON^- complex at 1370 cm^{-1}, which is in the N−O stretching mode region of Ni:NO (A) species. The question of possible differences in charge-transfer effects between end-on and cyclic forms will be discussed in the next section, with the results of quantum chemical calculations.

4. Theoretical Study of the NiNO Complex

In a first step, the energetical, geometrical and vibrational properties of NO are computed and compared to known experimental data.[24] These are reported in Table 4 along with the electronic energies of Ni in the triplet ground state.

A former study at the CASSCF level had calculated a binding energy in a linear Ni−N═O configuration 50% larger than in a bent configuration.[25] In the two recent DFT systematic studies on series of M−NO complexes (where M is a first row transition atom), results pertaining to one energy minimum were presented. It corresponds to a bent configuration (136 and 137° in refs 8 and 9, respectively).

In a second step, we have computed at the same level of calculations, energetical, geometrical and vibrational properties for the Ni−N═O bent form ^{2}A′ state (Table 5). Our results for higher spin multiplicities are in agreement with the results of Blanchet et al.;[9] the quartet state lies about 1 eV higher in energy and has not been considered further here. The inclusion of larger basis sets in this study results into slightly shorter bond lengths at every level of calculation and minor differences in predicted vibrational properties with respect to ref 8. A closer agreement is obtained between the results of ref 9 and those obtained here with B3LYP and B3PW91.

From the experimental results presented here, it appears clearly that another, isomeric or metastable form must exist, energetically competitive but separated by a sizable energy barrier from the former form. We have therefore undertaken a systematic exploration of the Ni−NO energy surface, without imposing geometry constraint. It appears that a second energy minimum exists at every level of calculation, which correspond to a drastically different structure, with an acute ∠NiNO bond angle, that is, a side-on configuration.

In Table 6 are presented energies, geometries and vibrational properties for the second form (^{2}A″) along with the optimized geometry and energies corresponding to the transition state (TS) between ^{2}A′ and ^{2}A″ structures. These results confirm the existence of a second, pseudo-cyclic structure.

For both forms the calculated frequency shifts ($\nu_{NO} - \nu_{NiNO}$) on the NO stretching mode (ν_1) are in better agreement with

TABLE 7: Topological Properties of NO and NiNO Isomers

	q_{Ni}	q_N	q_O[a]	$\rho(r_c)$[b]	$\nabla^2\rho(r_c)$	$H(r_c)$[c]	r_c[d]
NO							
(B3PW91)		−0.094	+0.094	0.595	−1.976	−1.035	N−O
NiNO (A′)				0.543	−1.460	−0.803	N−O
B3PW91	0.390	−0.350	−0.040	0.183	+0.715	−0.098	Ni−N
NiNO (A″)				0.450	−0.865	−0.555	N−O
B3PW91	0.690	−0.180	−0.510	0.134	0.401	−0.062	Ni−N
NiNO (A″)				0.420	−0.638	−0.473	N−O
BPW91	0.667	−0.147	−0.520	0.145	+0.403	−0.070	Ni−N
				0.111	+0.660	−0.031	Ni−O

[a] Mulliken atomic charges. [b] $\rho(r_c)$ = electron density at each bond critical point $\nabla\rho(r_c) = 0$. [c] $H(r_c)$ = local energy density at r_c. [d] Bonds for which critical points are found.

experiment for the pure functional than for the hybrid functional methods. This trend was already noted by Ruschel at al.[8] As shown in Tables 5 and 6, the Ni−NO stretching frequency is calculated, when using pure DFT functionals, slightly larger than the experimental value, while the reverse trend exists using the hybrid functionals. As discussed by Barone,[26] hybrid methods are thought to give slightly more realistic values for the binding energies than pure DFT functionals, and thus for the calculation of the energy barrier, the B3PW91 results were retained (Table 6). Using either method, one notes that the binding energy of the side-on form is about two-third that of the most stable bent end-on configuration. At the B3PW91 level, the barrier height for $^2A'' \rightarrow {}^2A'$ isomerization corresponds to about 4 kcal/mol, for an energy difference of about 11.5 kcal/mol (these values are uncorrected for zero point energies, and are anyway expected to be rough estimates).

The computed IR intensities for each form are in qualitative agreement with experiment. The NO stretching modes are by far the most intense in each species, but is much weaker in the cyclic form than in the end-on bent form. Also the low-frequency stretching and bending modes are one to two orders of magnitude less intense, and the weakest predicted band of all (ν_3 of $^2A'$ NiNO) could not even be detected in our experiments. For one form, the most stable configuration $^2A'$, the agreement between predicted and experimental properties looks however deceptively better than it really is. When the isotopic effects are calculated with the ab initio-derived force field, the $^{14}N/^{15}N$ and $^{16}O/^{18}O$ isotopic shifts are not correctly reproduced for the low-frequency modes, at every level of theory. The errors on the calculated isotopic shifts are as large as 40%, because the trends on the nitrogen and oxygen isotopic effects are reversed. A closer scrutiny of the force constants indicated that Ni−N force constant is underestimated and that of the bond angle bending overestimated. It results two frequencies having about the correct frequencies, but the computed normal modes are different of what can be inferred from the semiempirical calculations. This might be indicative of a slight underestimation of the Ni−N interaction for this form. Note that this discrepancy does not exist for the second, cyclic isomer $^2A''$, for which ab initio and semiempirical force fields are in quantitative agreement.

To help understanding the differences in bonding between the two isomers of NiNO, we have also examined the repartition of electronic charge density, and its Laplacian $\nabla^2\rho$ (at each bond critical point, where $\nabla\rho = 0$), using the topological method developed by Bader[27] (Table 7). First, the comparison of the computed Mulliken atomic charges shows in both complexes a substantial charge transfer from metal to nitrosyl ligand. This could be expected in view of the large permanent dipole moment appearing in either form (above 2 and 4.5 D in NiNO A′ and A″, respectively, versus only 0.15 D in NO), but the charge transfer is substantially greater in the metastable cyclic A″ form than in the end-on configuration A′. This could help stabilizing the former in a weakly polarizable medium such as here solid argon. For either form $\nabla^2\rho(r_{NO})$ is reduced from the free NO value, but the decrease is drastic for the $^2A''$ form. Note that the $\nabla\,{}^2\rho(r_{Ni-N})$ are positive in both cases, a result associated with predominantly closed shell interactions,[27] but according to another criterion proposed by Cremer,[28] a negative sign of the local energy density $H(r_c)$ at the bond critical point is indicative of a partly covalent bond.

An onset of Ni−O covalent bonding appears more clearly in the BPW91 results for the $^2A''$ cyclic structure (the Ni−N and Ni−O bond distance are comparable, 1.79 vs 1.86 Å) which reveals a third bond critical point, nevertheless with a more clearly marked polar character.

5. Conclusions

Infrared spectra of Nickel mononitrosyl complexes isolated in solid argon have been reinvestigated. Analyses of the $^{58}Ni/^{60}Ni$, $^{14}N/^{15}N$, and $^{16}O/^{18}O$ isotopic effects indicate the existence of two isomeric forms of NiNO: one with an end-on bent configuration already observed by Ruschel et al.[8] and a second form with a cyclic structure, in which the NO ligand is significantly more perturbed. The structures and electronic properties of these two forms have also been calculated using DFT methods and the isomerization energies have been estimated.

The existence of several isomers of MNO species had already once been established by Tevault and Andrews,[29] for M = Li, although the open chain conformer was then thought to be coordinated through the oxygen atom. Recently Zhou and Andrews discuss the existence of two Cr + NO adducts, one with linear structure characterized by the two stretching modes at 1614 and 514 cm^{-1}, and a second species, presumably cyclic, responsible for a lower frequency NO stretching mode at 1108.8 cm^{-1} and two low-frequency bands at 528 and 478 cm^{-1}.[30] For the related, room-temperature stable species C_5H_5NiNO, Crichton and Rest had produced through UV irradiation a second isomeric form, characterized by a much lower NO stretching frequency than in the C_{5v} form (1390 versus 1838 cm^{-1}) which they assigned to a more ionic $(C_5H_5)Ni^+NO^-$ form, without being able to discuss the geometry charge quantitatively.[31] Thus, the existence of low lying isomeric forms with side-bonded nickel−nitrosyl coordination could also be considered for coordinatively saturated species.

References and Notes

(1) Frenz, B. A.; Enemark, J. H.; Ibers, J. A. *Inorg. Chem.* **1969**, 8, 1288.
(2) Jones, L. H.; McDowell, R. S.; Swanson, B. I. *J. Phys. Chem.* **1973**, 58, 3757.
(3) Fisher, E. O.; Jira, R. *Z. Naturforsch.* **1954**, 96, 618.
(4) Cox, A. P.; Brittain, A. H. *J. Chem. Soc., Faraday Trans I.* **1969**, 557.
(5) Feltham, R. D.; Fateley, W. G. *Spectrochim. Acta* **1964**, 20, 1081.
(6) Wilkinson, G. *Comprehensive Coordination Chemistry*; Pergamon Press: Oxford, 1987; Vol. 5.
(7) Matsui, R.; Semba, K.; Honma, K. *J. Phys. Chem.* **1997**, 101, 179.
(8) Ruschel, G. K.; Nemetz, T. M.; Ball, D. W. *J. Mol. Struct.* **1996**, 384, 101.
(9) Blanchet, C.; Duarte, H. A.; Salahub, D. R. *J. Phys. Chem.* **1997**,-106, 88778.
(10) Joly, H. A.; Manceron, L. *Chem. Phys.* **1998**, 226, 61.
(11) Manceron, L.; Alikhani, M. E.; Joly, H. A. *Chem. Phys.* **1998**, 228, 73.
(12) Krim, L.; Lacome, N. *J. Phys. Chem.* **1998**, *102*, 2289.
(13) Clusius, K. *Angew. Chem.* **1954**. 66. 497.
(14) Frisch, M. J.; Trucks, G. W.; Schlegel, H. B.; Gill, P. M. W.; Johnson, B. G.; Robb, M. A.; Cheeseman, J. R.; Keith, T.; Petersson, G. A.; Montgomery, J. A.; Raghavachari, K.; Al-laham, M. A.; Zakrzewski,

V. G.; Ortiz, J. V.; Foresman, J. B.; Cioslowski, J.; Stefanov, B. B.; Nanayakkara, A.; Challacombe, M.; Peng, C. Y.; Ayala, P. Y.; Chen, W.; Wong, M. W.; Andres, J. L.; Replogle, E. S.; Gomperts, R.; Martin, R. L.; Fox, D. J.; Binkley, J. S.; Defrees, D. J.; Baker, J.; Stewart, J. P.; Head-Gordon, M.; Gonzalez, C.; Pople J. A. *Gaussian 94*, Revision D.4; Gaussian, Inc.: Pittsburgh, PA, 1995.

(15) Becke, A. D. *J. Chem. Phys.* **1993**, 98, 5648.

(16) Lee, C.; Yang, W.; Parr, R. G. *Phys. Rev. B*, **1988**, 37, 785.

(17) Perdew, J. P.; Wang, Y. *Phys. Rev. B*, **1992**, 45, 13244.

(18) McLean, A. D.; Chandler, G. S. *Chem. Phys.* **1980**, 72, 5639. Krishnan, R.; Binkley, J. S.; Seeger, R. Pople, J. A. *J. Chem. Phys.* **1980**, 72, 650.

(19) Schaefer, A.; Huber. C.; Ahlrichs, R. *J. Chem. Phys*. **1994**, 100, 5829.

(20) Canty, J. F.; Stone, E. G.; Bach, S. B. H.; Ball, D. W. *Chem. Phys*. **1997**, 216, 81.

(21) Manuscript to be published.

(22) Chiarelli, J. A.; Ball, D. W. *J. Phys. Chem*. **1994**, 98, 12828.

(23) Andrews, W. L. S.; Pimentel, G. C. *J. Chem. Phys*. **1966**, 44, 2361.

(24) Huber, K. P.; Herzbeg, G. *Molecular spectra and Molecular structure constant of Diatomic Molecules*; Van Nostrand Reinhold: New York, 1979.

(25) Bauschlicher, Jr. C. W.; Bagus, P. S. *J. Chem. Phys.* **1984**, 80, 944.

(26) Barone, V. *Chem. Phys. Lett*. **1997**, 216, 81.

(27) Bader, R. F. *Atoms in Molecules, A Quantum Theory*; Oxford University Press: Oxford, 1994.

(28) Kraka, E.; Cremer, D. *J. Mol. Struct.* **1992**, 255, 189 and references therein.

(29) Tevault, D. E.; Andrews, L. *J. Phys. Chem*. **1973**, 77, 1640.

(30) Zhou, M.; Andrews, L. *J. Phys. Chem*. **1998**, 102, 7452.

(31) Crichton, O.; Rest, A. *J. Chem. Soc., Chem. Commun.* **1973**, 407.